Journal of Building Engineering 44 (2021) 102972

Contents lists available at ScienceDirect

Journal of Building Engineering

journal homepage: www.elsevier.com/locate/jobe

Regional standardized particle size distributions for developing a Chinese filter testing standard used in building ventilation

Huayuan Zhou [a], Yang Sun [b], Ke Zhong [a], Yuesi Wang [b], Jie Cai [c], Yanming Kang [a,*]

[a] School of Environmental Science and Engineering, Donghua University, Shanghai, 201620, China
[b] Institute of Atmospheric Physics, Chinese Academy of Sciences, Beijing, 100029, China
[c] Chinese Contamination Control Society, Beijing, 100840, China

ARTICLE INFO

Keywords:
Particle size distribution
Indoor air quality
Air filter
Collection efficiency
Building ventilation

ABSTRACT

The impact of particulate matter (PM) on indoor air quality (IAQ) has become an important issue in China, whereas the standard for the filtration of PM in building ventilation has not been promulgated up to now. Due to the impacts of particle size distribution (PSD) on the particle removal efficiency of the air filters, and also due to the various characteristics of local PSD across China, it is necessary to analyze the selection of PSD when evaluating particle removal efficiency for practical applications. Although the efficiency of PM (ePM_X) for various particle size ranges, proposed in the latest EN ISO 16890 standard, is used to evaluate the actual effect of air filters for building ventilation on the improvement of IAQ, it is inappropriate to be adopted for the cases in China. In the present study, fine particle proportion ($PM_{2.5}/PM_{10}$) is employed and ambient aerosol distributions across China are analyzed. The measured PSDs at 35 cities are fitted to bimodal distribution. And then the ePM_X and class reporting values (CRVs) of three representative filters are calculated. The results indicate that being affected by the characteristics of PSD, the ePM_X and CRV differences of the same air filter between different PSD regions can be up to about 20% and 15%, respectively. Therefore, the China PSD regions are divided into five regions and the standardized PSD is determined for each region of the mainland.

1. Introduction

Over the past decade, indoor air quality (IAQ) has been a global concern of the government, the public and the scientific community [1–4]. One of the most significant parameters for evaluating IAQ in new and existing buildings is $PM_{2.5}$ (or PM_{10}) [1], which can be promisingly eliminated by air filters in fresh air units for building ventilation. As one of the main sources of indoor particle, high outdoor particulate matter (PM) concentration has significant impacts on indoor environment. Therefore, the accurate evaluation of particle (i.e., $PM_{2.5}$ or PM_{10}) removal efficiency of the air filters plays a crucial role in maintaining a good IAQ. Moreover, according to aerosol dynamic theory [5], particle size distribution (referred to as PSD, hereinafter) of outdoor air also has large impacts on the estimation of particle removal efficiency.

The PSDs are affected by climate and local economic development level [6]. China covers a vast geographical area (approximately 9.6 million square kilometers) with a wide variety of climates, including monsoon climate, plateau and alpine climate, and continental climate. In addition, the levels of economic development and process of urbanization vary significantly from place to place. Particularly, the average gross regional products of East China in 2018 was over three times than that of West China [7]. These differences in climate and local economic development level among different regions lead to diverse characteristics of PSD in different regions of China. For example, Song et al. [8] observed the aerosol distribution of China from 2014 to 2016 and found that the ratio of fine particle ($PM_{2.5}/PM_{10}$) in Shanghai is 87.5% higher than that in Lanzhou.

Although PSDs may vary greatly between cities in China, neither the design of building ventilation systems nor the filter classification can be standardized if a local PSD is assumed in each city to calculate particle removal efficiency of the fresh air filter. On the other hand, if only one "standardized" PSD is used across the country, particle removal efficiency of the filter will be inevitably overestimated or underestimated due to the regional differences in the local PSDs, and this will result in the risk that the quality of fresh air which is cleaned by the filters and delivered into the interior space fails to reach the design requirement. To cope with this dilemma, the notion of climate region for building thermal design [9] can be adopted as a reference. Similarly, the notion of

* Corresponding author.
E-mail address: ymkang@dhu.edu.cn (Y. Kang).

https://doi.org/10.1016/j.jobe.2021.102972
Received 10 April 2021; Received in revised form 26 June 2021; Accepted 9 July 2021
Available online 11 July 2021

China PSD region may be a reasonable solution.

It is noted that a new international filter testing standard, EN ISO 16890-1:2016 standard [6] (referred to as ISO 16890, hereinafter), has established an efficiency classification system of air filter for building ventilation based upon particulate matter that can be used as the basis for China PSD region. The efficiency of particulate matter, i.e., ePM_X (including ePM_1, $ePM_{2.5}$ and ePM_{10}), for various particle size ranges is employed in ISO 16890. The filter classes are reported as class reporting value (CRV), rounded downwards to the nearest multiple of 5% points, rather than continuous values. This standardized treatment of ePM_X, characterized by step, can act as guideline for China PSD region.

In the present study, the monitored outdoor aerosol concentrations in different regions of China are used to analyze the ambient aerosol characteristics across China. The classification system in ISO 16890 and the local particle removal efficiencies of representative filters at 35 cities are employed to propose several principles for China PSD region. And then the PSDs are divided into different types with the same ambient aerosol characteristics within groups. Finally, the standardized PSD is defined in each China PSD region to provide theoretical basis and data support for standardization of filter system design for building ventilation in different regions of China. Technical route of this work is shown in Fig. 1.

2. Analysis of ambient aerosol monitoring results in China

2.1. Particulate matter data source

$PM_{2.5}$ and PM_{10} have been monitored continuously at more than 1300 national air quality monitoring sites (NAQMSs) in 31 provinces of China by the Institute of Atmospheric Physics, Chinese Academy of Sciences. As shown in Fig. 2, the blue squares represent the geographical distributions of NAQMSs, and the red line is the Hu Huanyong Line (i.e. the Hu Line), an imaginary line stretching from Heihe (a northern city of China near the border of China and Russia) to Tengchong (a southwestern city of China bordering with Myanmar), which divides the area of China into two roughly equal parts [10]. The Hu Line shows an uneven geographical pattern of urbanization which is characterized by a dense population and rapid urbanization in the eastern area and sparse population and slow urbanization in the western area [10]. These NAQMSs not only cover four mega-city clusters (Beijing-Tianjin-Hebei, Yangtze River Delta, Pearl River Delta, and Cheng-Yu), but also include major cities in the inland of China, such as Xi'an, Lanzhou and Urumqi, to better understand the spatial variations in PM concentrations across China.

Each NAQMS was equipped with a TEOM RP1400a$-PM_{2.5}/PM_{10}$ with a 0.1 $\mu g/m^3$ resolution, precisions of ± 1.5 $\mu g/m^3$ (1-h average) and ± 0.5 $\mu g/m^3$ (24-h average), and a 0.06 $\mu g/m^3$ (1-h average) minimum detectable limit [11,12]. The filters were replaced every two weeks, and the flow rates were monitored and calibrated every month. The sampling interval was 15 min. The installation, setting and maintenance of monitoring instruments were carried out in accordance with the ministry-level standard of "Automated methods for ambient air quality monitoring" (HJ/T 193–2005) [13]. To investigate the current status of PM distributions and analyze the spatiotemporal characteristics of PM in China, $PM_{2.5}$ and PM_{10} mass concentrations of every hour were gathered from January 2016 to December 2018.

2.2. Temporal variations of particulate matter

It has been reported that both anthropogenic emission and meteorological conditions have evident seasonal differences between the regions [14]. According to Chinese heating policy [9], coal-based centralized heating is employed only in winter, so both $PM_{2.5}$ and PM_{10} have a clear boundary between heating and non-heating periods [15]. Besides, monsoon climate results in different sources of PM in different seasons, i.e., the PM primarily comes from the ocean in summer and the inland in winter. Fig. 3 shows the temporal variation of statistical characteristics of the particle mass concentrations from 2016 to 2018 at four representative cities.

As can be seen from Fig. 3, regardless of whether coal-based centralized heating is employed in these four cities, the PM mass concentrations in winter were significantly higher than those in other seasons. This is because meteorological conditions in winter, such as low boundary layer height, weaker winds, less precipitation and lower temperature, compared with those in other seasons, can further exacerbate air pollution [16]. In addition, the monitoring data showed a similar pattern occurred in other cities. The findings are consistent with the results by Ref. [17]. Provided that air filters are selected and equipped based on the PM concentration in winter (i.e., under high-pollution conditions), the IAQ will also be satisfactory in other

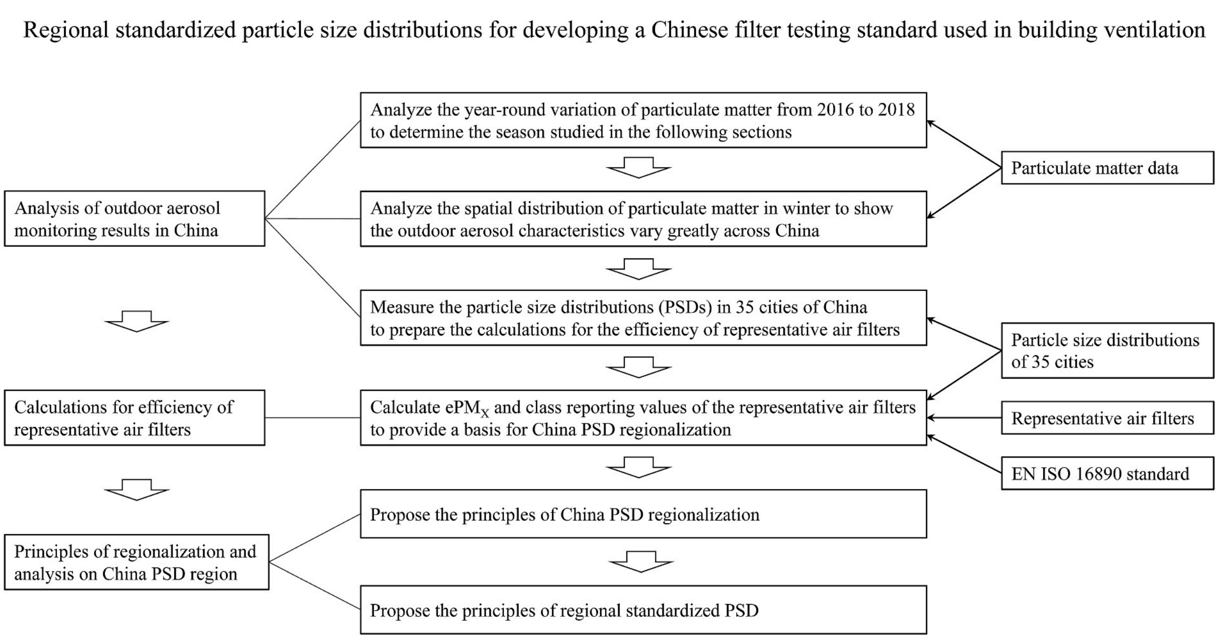

Fig. 1. Technical route of this study.

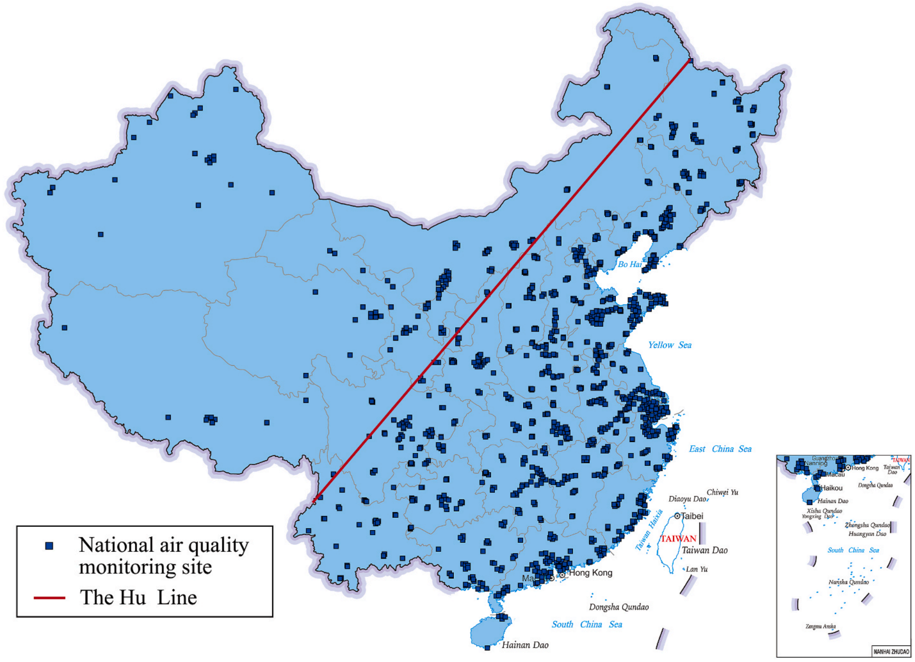

Fig. 2. Geographical distributions of national air quality monitoring sites.

seasons (i.e., under low-pollution conditions). Therefore, only the PM concentrations in winter (instead of the whole year) will be analyzed in the following sections considering the most severe pollution situation in winter.

2.3. Spatial distributions of particulate matter in winter

Air pollution is more severe in provincial capital cities or major cities than in other cities [18], and the population in these cities is also denser compared with those in other cities [7]. In addition, the demand of the air filters in fresh air system is higher in these cities than in others. In this study, the heavily polluted provincial capital cities or major cities are considered as the typical cities of the corresponding provinces for the analysis because severe pollution results in health risks. Fig. 4 shows the spatial distribution of the average PM_{10} and $PM_{2.5}$ concentrations at provincial capital cities in the winter from 2016 to 2018.

Fig. 4 shows very similar results by Fan et al. [17] and Song et al. [8] who also found that the average $PM_{2.5}$ and PM_{10} concentrations varied greatly among different regions. Comparing the results in Fig. 4(a) and (b), the spatial distributions of $PM_{2.5}$ and PM_{10} were similar in the most regions, except for Xining and Lanzhou (see the red circles in Fig. 4) with low $PM_{2.5}$ and high PM_{10}, and Harbin with high $PM_{2.5}$ and low PM_{10}. This suggests that the ambient aerosol characteristics across China are obviously different from region to region due to diverse anthropogenic emissions and meteorological conditions for atmospheric dispersion and dilution.

Considering that the proportion of $PM_{2.5}$ to PM_{10} can roughly characterize the percentage of fine particles (or coarse particles) in a region, the ratio of the mass concentration of $PM_{2.5}$ to PM_{10} is defined as the fine particle proportion (FPP), η_f, which is given by

$$\eta_f = \frac{C_{2.5}}{C_{10}} \tag{1}$$

where the C_{10} and $C_{2.5}$ are the mass concentrations of PM_{10} and $PM_{2.5}$, respectively.

In order to analyze the variations of FPPs, Fig. 5 shows the scattering distributions of FPPs in nine typical cities by using the hourly-averaged data in the winter from 2016 to 2018. These nine cities can represent the eastern, central, western and coastal regions of China to a definite extent, and these cities are also the main economic cities of mega-city clusters in China.

It is found from Fig. 5 that the FPPs in the nine cities varied within a wide range during the measurement. Because the averaged FPP is affected by extreme values of the data and easily deviates from its reasonable value, the median of fine particle proportion (MP), denoted as η_m, is used for the following analysis.

Due to the humid climate in a whole year, the MPs of Shanghai, Wuhan and Chongqing were high and almost the same ($\eta_m = 0.78$). Influenced by sea-salt aerosol, the MPs of Guangzhou (near the South China Sea) and Xiamen (with a long coastline) were very close ($\eta_m = 0.65$). The MPs of Lanzhou and Xi'an (in arid region) were quite low, being approximately 0.58. Due to the slow economic development and the original ecology environment in Lhasa, the MP was the lowest among the nine cities, being only about 0.43.

In order to directly show the spatial distribution of MPs, Fig. 6 depicts the spatial distribution of the MPs in each provincial capital city.

As can be seen from Fig. 6, there are obvious regional differences of MPs in different regions of China. The highest MPs (about 0.8) that occurred in Changsha and Harbin were twice higher than the MP in Lhasa. In contrast, the lowest MPs existed in the northwest of China, ranged approximately from $\eta_m = 0.4$ to $\eta_m = 0.5$, meaning that coarse particles accounted for most of PM_{10}, whereas there were more fine particles in South and East China. These results match that observed by the previous study [8].

Fig. 7 shows the delineation of climate regions and moisture regions of China [9]. The low MPs in the northwest of China, located in the typical temperate (semi-)arid region, which features sparse vegetation, desertification and is close to the deserts, are mainly attributed to mineral aerosol emission caused by dust storms. The humid climates in East and South China with abundant rainfall lead to high MPs. In addition, coastal regions with monsoon climates are not only affected by local anthropogenic emissions but also by sea-salt aerosols. The completely different climatic characteristics and different local anthropogenic activities cause the significantly different ambient aerosol characteristics, i.e., PM pollution is dominated by fine particles in some regions but coarse particles in other regions. Therefore, the ePM_X of the same filter may vary considerably with different ambient aerosol characteristics. The ambient aerosol characteristics in China first should be

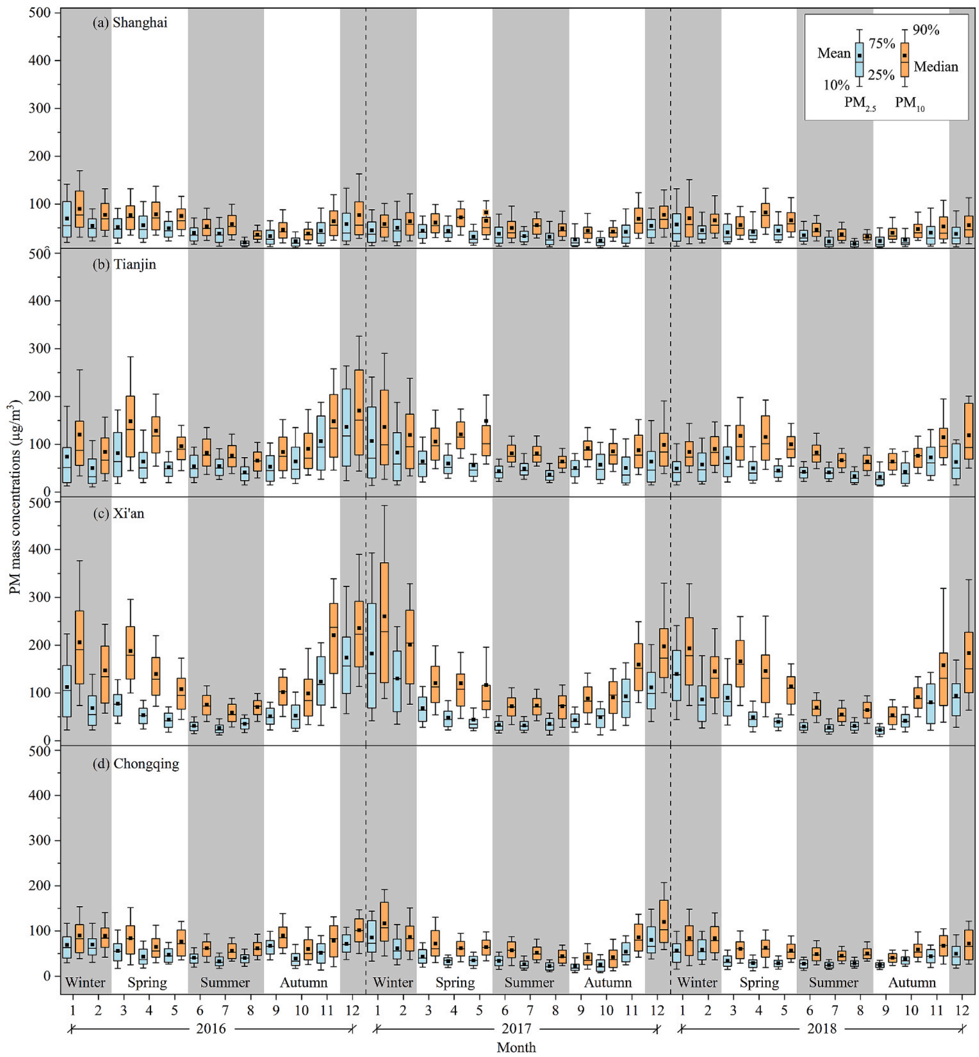

Fig. 3. Temporal variation of statistical characteristics of particle mass concentrations from 2016 to 2018 (Note: 10%, 25%, 75% and 90% represent different confidence levels of the samples).

divided into several groups with similar patterns and trends within groups when ISO 16890 is introduced to China.

2.4. Identification of particle size distributions in 35 cities

The PSDs in 35 major cities of China have been monitored by the Institute of Atmospheric Physics, Chinese Academy of Sciences. The monitoring instrument was a cascade impactor (Andersen Series 20–800) [19]. The flow rate of vacuum pump was 28.3 L/min and the sampler had nine size stages with nominal cut-off set, i.e., $d < 0.4$, 0.4–0.7, 0.7–1.1, 1.1–2.1, 2.1–3.3, 3.3–4.7, 4.7–5.8, 5.8–9, and $d > 9$ μm.

The actual particle mass frequencies *versus* cut-off diameters, denoted as $q_i(d)$, are calculated from the measured PM mass concentrations and the logarithmic width of the particle diameter size range, as is given by

$$q_i(d) = \frac{m_i}{M \cdot \Delta \ln d_i} \tag{2}$$

where i is the number of the channel (size range) of the impactor; m_i is the PM mass concentrations (μg/m^3) in the channel i and M is the total PM mass concentrations (μg/m^3), $\Delta \ln d_i = \ln d_{i+1} - \ln d = \ln(d_{i+1}/d)$.

The PSDs can be defined by curve fit from the actual particle mass frequencies $q_i(d)$. The fitted curve, referred to ISO 16890, is derived from the bimodal distribution by combining the lognormal distributions for the fine (A) and the coarse (B) mode, weighted with the mixing ratio, y, as can be expressed by [6]

$$q(d) = \frac{\mathrm{d}Q(d)}{\mathrm{d}\ln d} = y \cdot f(d, \sigma_{gA}, d_{50A}) + (1-y) \cdot f(d, \sigma_{gB}, d_{50B}) \tag{3}$$

where $f(d, \sigma_g, d_{50})$ represents the lognormal particle distribution function of ambient aerosol for one mode, coarse or fine, as given by

$$f(d, \sigma_g, d_{50}) = \frac{1}{\ln \sigma_g \cdot \sqrt{2\pi}} \cdot \exp\left[-\frac{(\ln d - \ln d_{50})^2}{2 \cdot (\ln \sigma_g)^2} \right] \tag{4}$$

where σ_g is the standard deviation and d_{50} is the median optical diameters, both are the scaling parameters.

Fig. 8 plots a diagram of the fitted PSDs in the 35 cities. The points are the actual particle mass frequencies measured in each city. A full list of fitting parameters for these fitted PSDs is shown in Table A.1. Fig. 8 suggests that the PSDs of all the cities are bimodal distributed with a fine and coarse mode but different from the PSDs proposed in ISO 16890. This is because that the PSDs in ISO 16890 were taken directly from the book on *Atmospheric Chemistry and Physics* by Seinfeld and Pandis [20]. Moreover, the urban PSD appears to come from two publications from the 1960s and 1970s [21,22]; the rural PSD given by Hobbs [23] are stated to come from the measurements conducted in 1975 and 1976 over

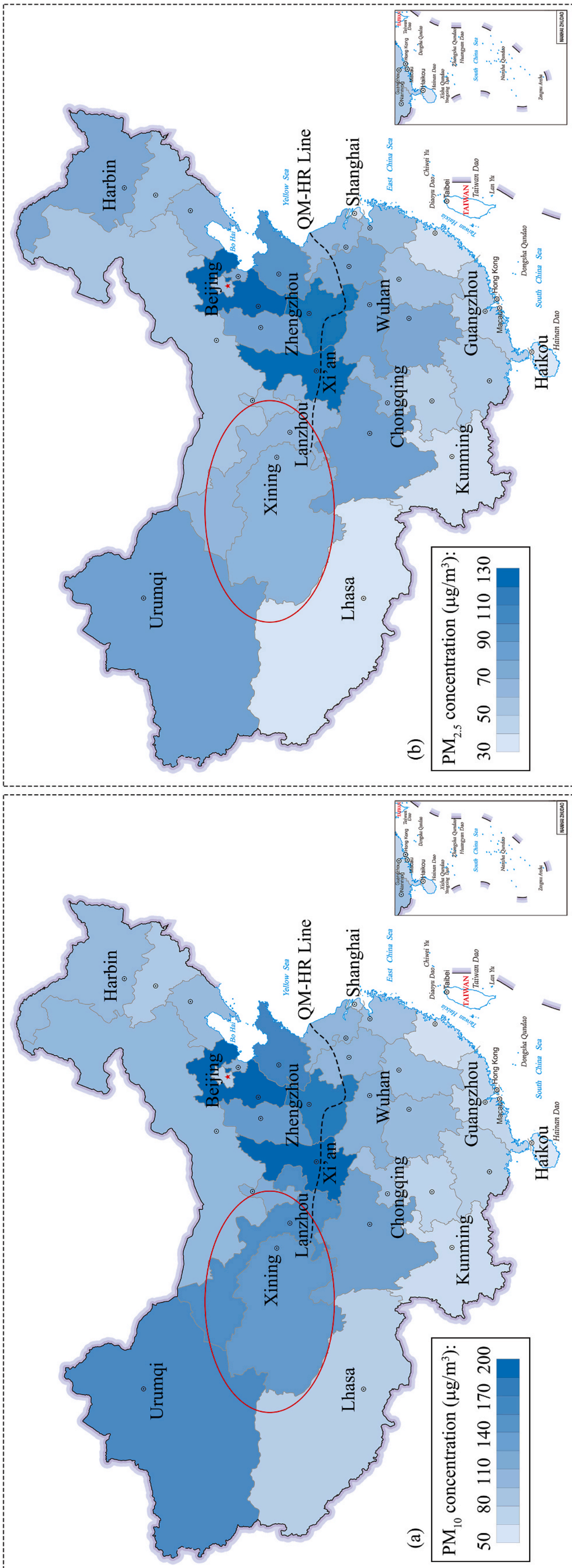

Fig. 4. Spatial distribution of the average (a) PM_{10} and (b) $PM_{2.5}$ concentrations in the winter from 2016 to 2018.

the high plains of North America [24]. In addition, the measured PSDs in some cities are in agreement with the results of previous studies on PSDs in Chinese cities [25–27]. The mixing ratio, y, the standard deviations, σ_g, and the median particle sizes, d_{50}, of PSD in each city are all different (see Table A.1 for specific data).

3. Calculations for ePM_X and class reporting values of representative air filters

3.1. Preparation of representative air filters for building ventilation and classification system based on ePM_X

According to the classification system in ISO 16890 [6], it is necessary to use the size-resolved removal efficiency curve of air filter. Therefore, a survey of domestic air filter of various classes and a statistical analysis of the size-resolved removal efficiency curves of these air filters have been conducted by the Chinese Contamination Control Society, Chinese Institute of Electronics in recent years. In this way, the typical removal efficiency curves of domestic air filters were obtained. The initial size-resolved removal efficiency curve, E_i, of the untreated and unloaded filter element and the size-resolved removal efficiency curve, $E_{D,i}$, after an artificial conditioning step [28], are used to calculate the average size-resolved removal efficiency curve, $E_{A,i}$, as given by [6]

$$E_{A,i} = 0.5 \cdot (E_i + E_{D,i}) \tag{5}$$

Three types of air filters, i.e., high test-dust-capacity filter G4, fiberglass filters M6 and F8 (according to EN 779), are regarded as the representatives of the coarse, medium and fine filters, respectively. The removal efficiency curves of the three representative filters are shown in Fig. 9.

Then ePM_X defined in ISO 16890 [6] are calculated by employing the average size-resolved removal efficiencies $E_{A,i}$ (Eq. (5)) and the PSDs (Eq. (3)):

$$ePM_X = \frac{\sum_{i=1}^{n} E_{A,i} \cdot q\left(\overline{d}_i\right) \cdot \Delta \ln d_i}{\sum_{i=1}^{n} q\left(\overline{d}_i\right) \cdot \Delta \ln d_i} \tag{6}$$

where $\overline{d}_i = \sqrt{d_i \cdot d_{i+1}}$ is the geometric mean diameter and $\Delta \ln d_i = \ln d_{i+1} - \ln d = \ln(d_{i+1}/d)$, i is the number of the channel (size range) of the particle counter under consideration, and n is the number of the channel (size range) which includes the particle size, X ($d_n < X < d_{n+1}$), where X = 10 μm for ePM_{10}, X = 2.5 μm for $ePM_{2.5}$ and X = 1 μm for ePM_1.

Additionally, the minimum efficiencies, $ePM_{2.5,min}$ and $ePM_{1,min}$, are calculated by [6]

$$ePM_{X,min} = \frac{\sum_{i=1}^{n} E_{D,i} \cdot q\left(\overline{d}_i\right) \cdot \Delta \ln d_i}{\sum_{i=1}^{n} q\left(\overline{d}_i\right) \cdot \Delta \ln d_i} \tag{7}$$

The initial arrestance, the three efficiency values (i.e., ePM_1, $ePM_{2.5}$ and ePM_{10}), and the minimum efficiency values (i.e., $ePM_{1,\ min}$ and $ePM_{2.5,\ min}$) shall be used to classify a filter in one of the four groups given in Table 1 [6].

The filter classes are reported as class reporting value (CRV) in conjunction with the group designation. For the reporting of the ePM_X classes, the CRVs shall be rounded downwards to the nearest multiple of 5% points. Values larger than 95% are reported as "> 95%". Examples of CRVs are ISO Coarse 60%, ISO ePM_{10} 60%, ISO $ePM_{2.5}$ 85%, and ISO ePM_1 > 95% [6].

3.2. ePM_X and class reporting values of the representative filters

Based on the size-resolved removal efficiency curves of the

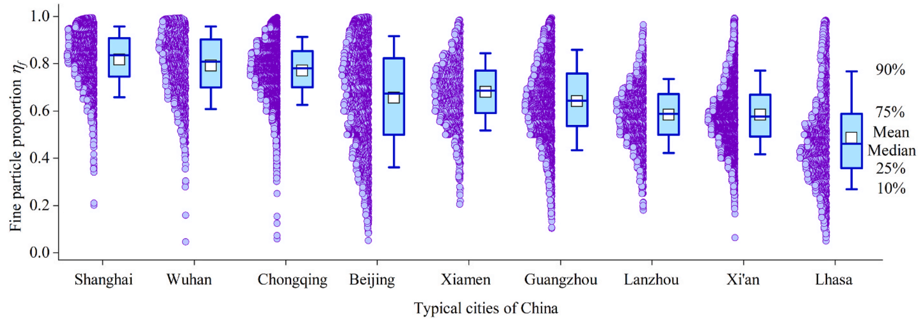

Fig. 5. Scatter diagram of fine particle proportions in typical cities of China.

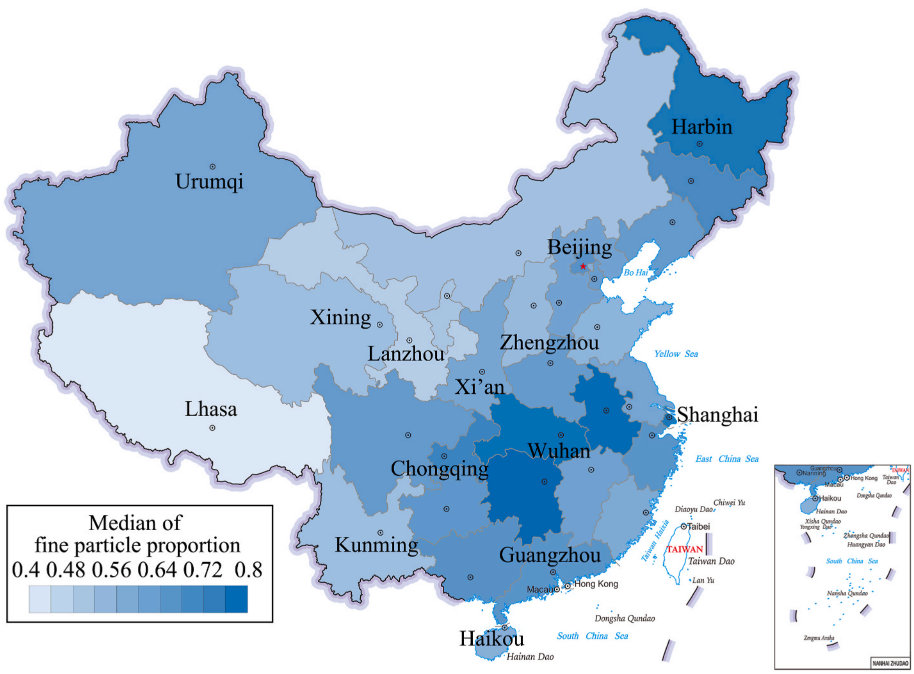

Fig. 6. Spatial distribution of the median of fine particle proportion in the winter from 2016–2018.

representative filters (see Fig. 9) and the PSDs in the 35 cities (see Table A.1), the ePM_X of the three representative filters in each city are calculated by Eq. (6). The ePM_X of the representative filters (see Table A.2 for specific data) are presented in roughly ascending order in Fig. 10.

From Fig. 10, it can be observed that the ePM_X of the same filter varied among the 35 cities due to the different PSDs in these cities. For example, the ePM_{10} of F8 are 87.8% in Nanjing, 90.6% in Chengdu, and 93.8% in Lhasa. In addition, PSDs have different influences on different ePM_X, with the least impact on ePM_1 and the greatest impact on ePM_{10}. Specifically, about 20% change of the ePM_{10} of M6 was caused by changes in PSDs between Shanghai and Kunming, but only 4% change of the ePM_1 of M6 occurred between them. Therefore, it must be addressed that the ePM_X of the same filter shows different values in different regions.

The CRVs, rounded from the calculated ePM_X, are depicted in Fig. 11. Because the ePM_{10} of G4 are higher than 50% only in Lhasa and Kunming, G4 can be identified as ePM_{10} 50% only in these two cities according to ISO 16890. However, it should be classified as the Coarse group (according to Table 1) if G4 is applied in the other 33 cities. Due to the lack of initial gravimetric efficiency of G4, the Coarse group will not be discussed in this study.

Depending on different PSDs in the 35 cities (in Fig. 8), there are several step points (tagged by red circles in Fig. 11) in most ePM_X classes of three representative filters, meaning that only one PSD is insufficient to represent the outdoor aerosol characteristics of China. Specifically, if the PSD measured in Beijing is used nationwide, the CRV of M6 will be 70%. The actual particle removal efficiency of M6, however, is 80% in Kunming and 65% in Shanghai, respectively.

On the other hand, the rounded CRVs in several cities were the same though the ePM_X were slightly different, which means that there is no need to define each standardized PSD for each province to assess and classify air filters. Consequently, standardized PSDs of China should be divided into several PSD regions with the same standardized PSDs within groups, so as not to overestimate or underestimate the particle removal efficiencies of air filters.

4. Principles and analysis on China particle size distribution region

4.1. Principles of regionalization and results of the China particle size distribution region

To determine the boundaries of the China PSD regions, the following principles are specified:

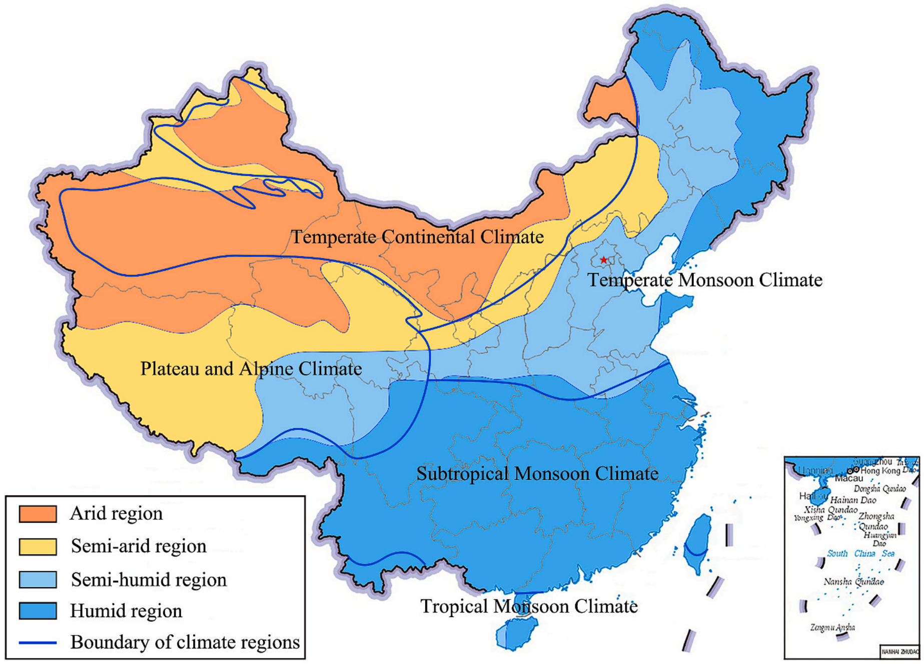

Fig. 7. Delineation of climate regions and moisture regions.

(1) Two step points (red circles in Fig. 11) must exist between the adjacent PSD regions (i.e., two different CRVs in the adjacent PSD regions) to avoid too many PSD regions.
(2) In order to keep the PM concentration indoors at a healthy level, for both the fresh air and returned-air cleaning, it is better to underestimate the particle removal efficiencies of air filters than to overestimate them. Thus, the second of the two step points between the PSD regions are regarded as the boundaries.

Based on the above principles, the PSDs are divided into five types of regions and the boundaries (black vertical dash dot lines) between two adjacent regions are shown in Fig. 11. The provinces and major cities included in each PSD region are listed in Table A.3. To visualize the geographical distribution of the PSD regions, the regions are marked in different colors on a map of China, with the result shown in Fig. 12.

Fig. 12 shows that Region 3 and Region 4 cover most of China. Region 1 is the region with the finest aerosols in China, including Heilongjiang and the Yangtze River Delta, where the climates are humid. There is heavy snowfall in winter in Heilongjiang with an average annual rainfall of about 500 mm. Additionally, the Yangtze River Delta is one of the most economically developed mega-city clusters in China, and has an extremely high level of urbanization, resulting in aerosols that are finer than those in any other regions of China. The provinces in Region 2 are Guizhou and Fujian in humid regions of South China and Beijing and Tianjin in North China. Beijing and Tianjin are located in a semi-humid region, and the human activities are also intense, so the aerosols are relatively fine. Region 3 includes not only some northwestern provinces, e.g., Ningxia and Gansu, with a dry climate and nondeveloped economy, but also some coastal provinces dominated by sea-salt aerosols, e.g., Shandong and Guangdong. In Region 4, the aerosols are relatively coarse, mainly in North China and West China, e.g., Qinghai and Shaanxi, located in desert areas or the transport pathways of Asian dust storms, which may be related to more frequent dust events, such as dust storm, floating dust, and blowing dust, originating from the upstream Taklimakan and Gobi Deserts [17]. Both Tibet and Yunnan are in Region 5, characterized by the coarsest aerosols, due to the natural atmospheric environment and slow urbanization.

4.2. Principles and results of standardized particle size distribution in each region

Though the CRVs in the same PSD region are rounded into the same values among the cities, the PSDs of each city are not exactly the same, and therefore the standardized PSDs of each region should be defined. The basic principle for determining the standardized PSDs is that the CRV rounded from the standardized PSD can only be underestimated but not overestimated, so the quality of outdoor fresh air, which is cleaned by the filters and then delivered into interior space, must be higher than the design level (or expected level). The specific principles are as follows:

(1) The city with the ePM_X minimum will be determined as the typical city of this region, and the measured PSD of this city will also be determined as the standardized PSD of this region to avoid overestimating the particle removal efficiencies of air filters.
(2) As far as national conditions and the public in China are concerned, the harm of $PM_{2.5}$ is the most remarkable at present for $PM_{2.5}$ can penetrate lungs. Therefore, the city with the $ePM_{2.5}$ minimum will be regarded as the typical city of the region, if the three ePM_X minima do not appear at the same city in one region (see specific data in Table A.2).
(3) In a filter system, a multi-stage filter system is generally designed and installed. Upstream filters, i.e., coarse and medium filters, are mainly used to protect fine downstream filters, so the PM concentrations in supply air are subject to the particle removal efficiencies of final filters. Thus, the city with the $ePM_{2.5}$ minimum of the highest level of filter is regarded as the typical city of the region, if the $ePM_{2.5}$ minima of different levels of the filters are at different cities in one region (see specific data in Table A.2).

The typical cities of each PSD region, according to these principles, are determined and the measured PSDs of these typical cities are considered as the standardized PSDs of the corresponding region. Table 2 lists the parameters for the standardized PSDs and the typical cities in each region, and Fig. 13 plots the standardized PSDs of each region.

The results in Fig. 13 clearly indicate the differences in the fine and

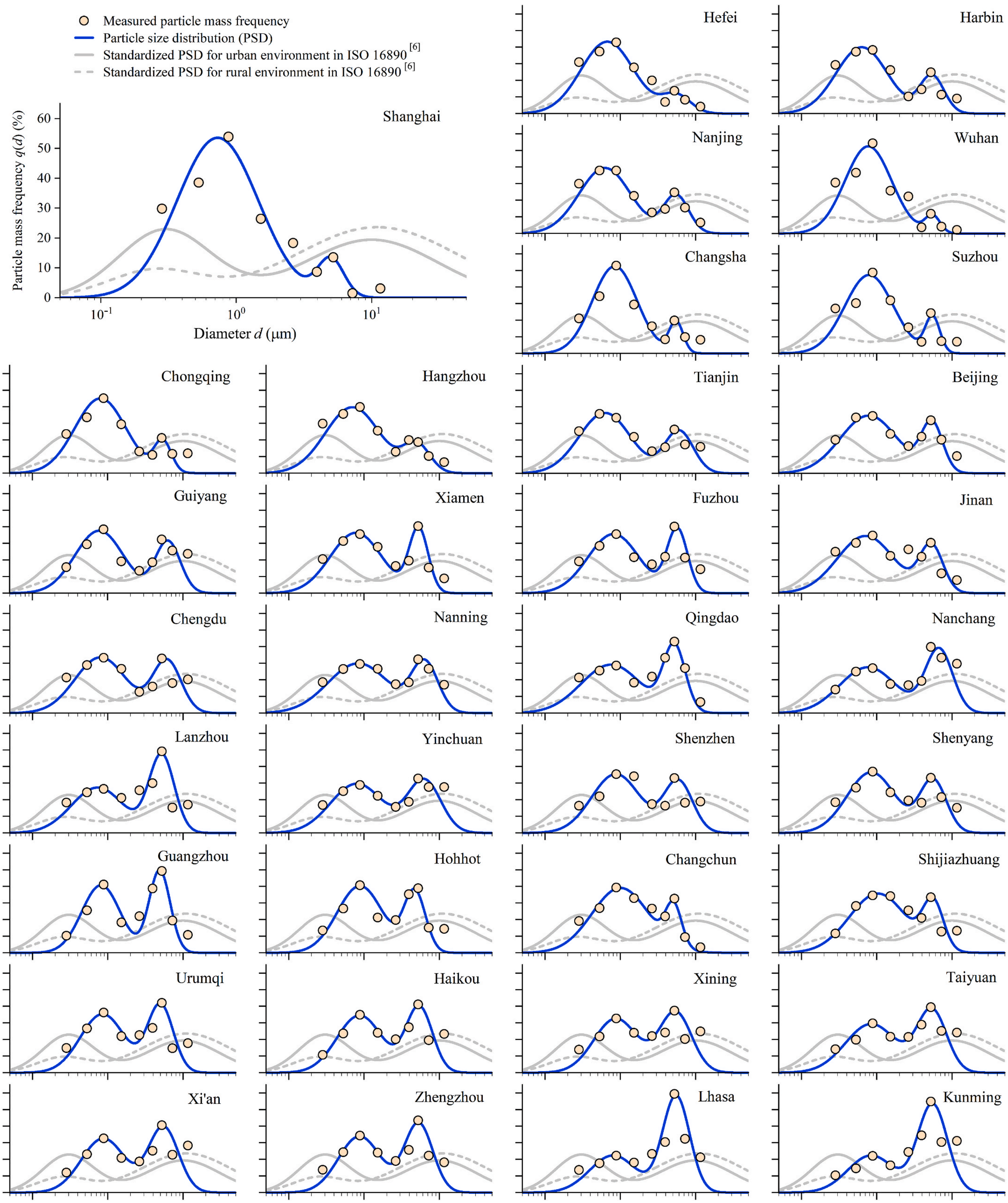

Fig. 8. Measured particle mass frequencies and the PSDs in 35 cities.

Table 1
Filter groups.

Group designation	Requirement			Class reporting value
	$ePM_{1,\,min}$	$ePM_{2.5,\,min}$	ePM_{10}	
ISO Coarse	–	–	<50%	Initial gravimetric arrestance
ISO ePM_{10}	–	–	≥50%	ePM_{10}
ISO $ePM_{2.5}$	–	≥50%	–	$ePM_{2.5}$
ISO ePM_1	≥50%	–	–	ePM_1

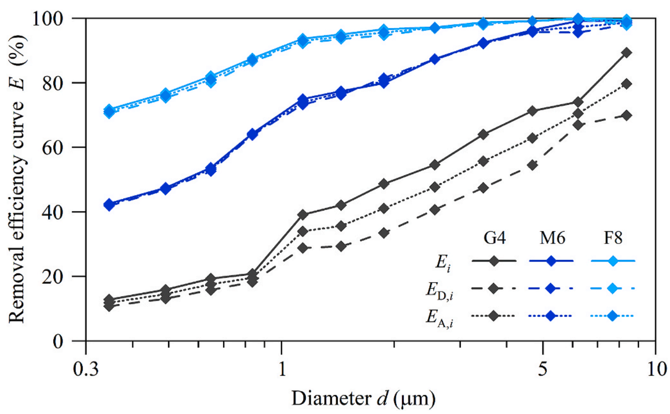

Fig. 9. Size-resolved removal efficiency curves of three representative filters.

Table 2
Parameters for the standardized PSDs and typical cities.

China PSD region	Parameters for the standardized PSDs					Typical cities
	y	σ_{gA}	d_{50A}	σ_{gB}	d_{50B}	
Region 1	0.78	2.20	0.64	1.47	5.50	Nanjing
Region 2	0.72	2.15	0.62	1.55	6.00	Tianjin
Region 3	0.60	2.38	0.76	1.52	6.70	Nanchang
Region 4	0.59	1.97	0.85	1.48	5.00	Urumqi
Region 5	0.40	2.04	0.80	1.51	5.50	Lhasa

coarse modes of the standardized PSDs between the PSD regions. The fine (coarse) modes of the standardized PSDs keep decreasing (increasing) with the increasing particle size from Region 1 to Region 5. In addition, the fine modes of the standardized PSDs in Region 1 and Region 2 are larger than the coarse modes, whereas the coarse modes in Region 3 to Region 5 are larger than the fine modes.

5. Discussion

To analyze the differences in ePM_1, $ePM_{2.5}$ and ePM_{10} of three representative filters in different PSD regions, Fig. 14 shows the CRVs of the three representative filters with the standardized PSDs of each region.

It can be seen from Fig. 14 that the coarse filter G4 can be classified as ePM_{10} 50% only in Region 5. As for the medium filter M6, the ePM_1 values in all PSD regions are the same, while the ePM_{10} values have considerable difference (up to 15%) between Region 1 and Region 5. In the case of the fine filter F8, notable difference (5%) can be observed in all three types of ePM_X between different PSD regions. Hence, these clear differences indicate the impact of different ambient aerosol characteristics on ePM_X and CRVs must be considered when ISO 16890 is introduced into China.

By comparing Fig. 14 with Fig. 11, it should be noted that the obtained CRVs with the standardized PSDs are less than or equal to the rounded CRVs with the measured PSDs, indicating that the typical cities and standardized PSDs are reasonable according to the above principles.

Obviously, standardization of the air filter testing and classification is undoubtedly important in the global air filtration market [29]. Because PSDs used in the calculation for ePM_X must represent the local ambient aerosol characteristics to precisely estimate the performance of air filter, the results by the present study can be used as a reference and assist other countries in adopting a suitable air filter testing standard to develop their national standard for the filtration and purification of PM in building ventilation.

The present study is subject to some potential methodological limitations. Due to high population density and demands of building fresh air systems, the cities with heavy air pollution are selected as typical cities, but these cities cannot represent the whole regions which they are located in. Therefore, these results are appropriate for these cities but may not be applicable to all situations. Moreover, many factors can affect the PSD regionalization in China, such as the changes of industrial structure and distribution, year-to-year variability of atmospheric aerosol species, differences in the accuracy of particle sampling instruments and filter-to-filter difference, which should be studied in further works.

6. Conclusions

With the increasing awareness of the importance of indoor air quality (IAQ), building ventilation has become an imperious demand in China. For the accurate evaluation of particle removal efficiency of air filters equipped in ventilation systems, it is necessary to analyze the impacts of particle size distribution (PSD) on the removal efficiency and the characteristics of PSD in different regions of China. In the present study, an integrated analysis of the spatial-temporal distribution characteristics of

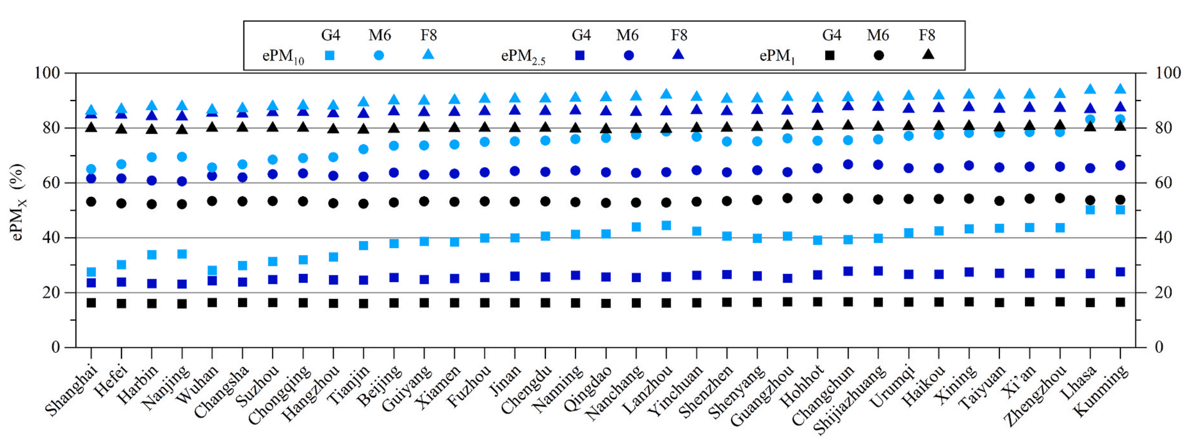

Fig. 10. ePM_X of the three representative filters in 35 cities.

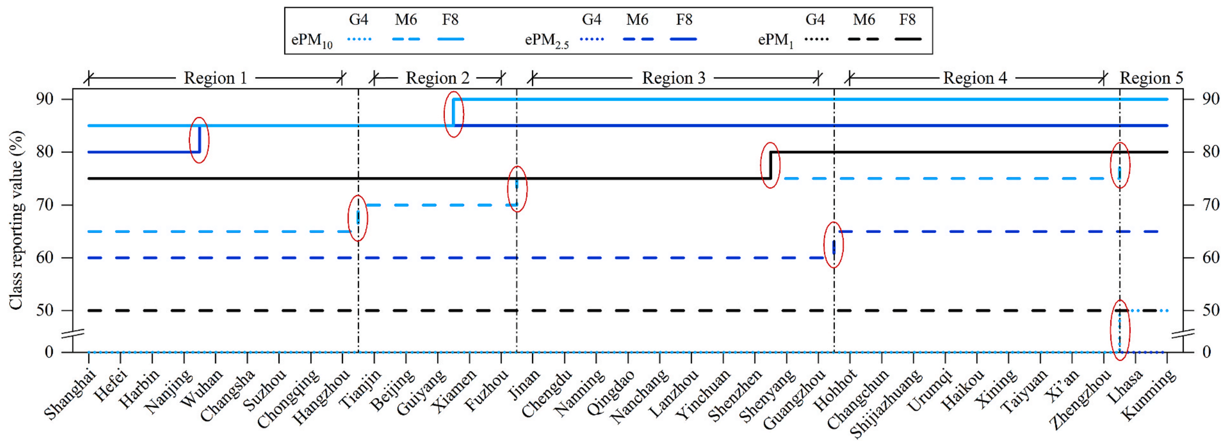

Fig. 11. Class reporting values of three representative filters in 35 cities.

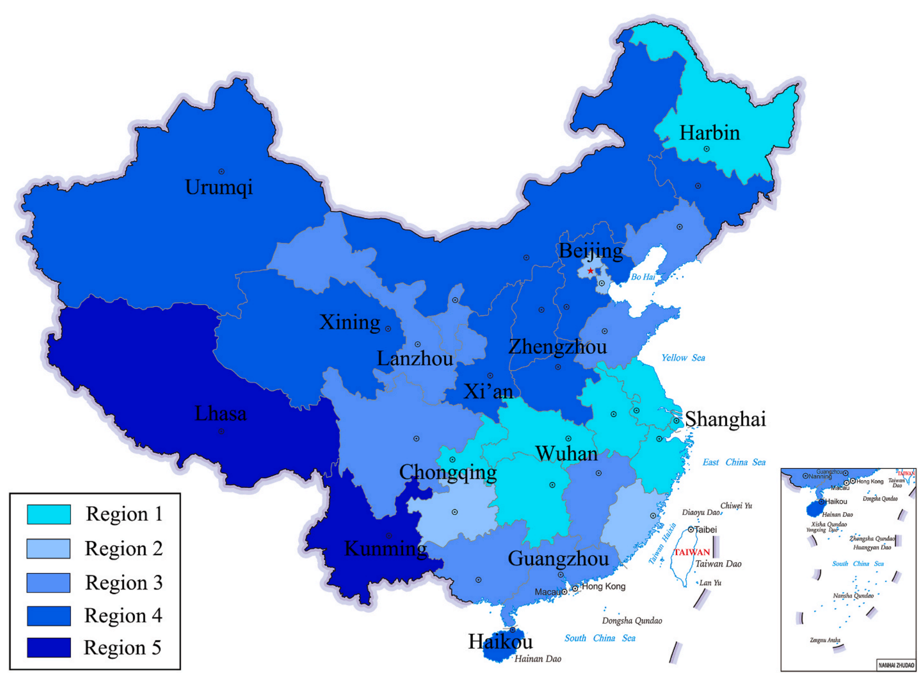

Fig. 12. Geographical distribution of China PSD regions.

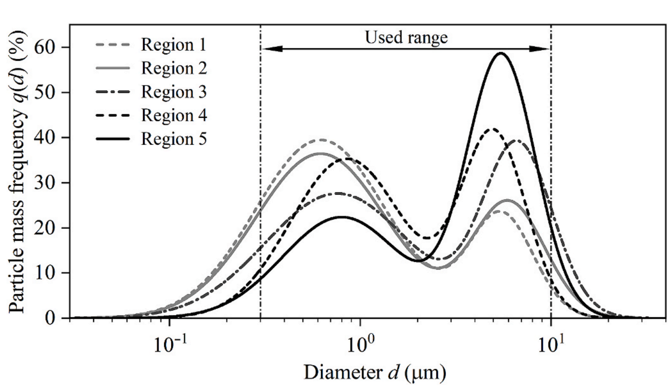

Fig. 13. Standardized PSDs of each region.

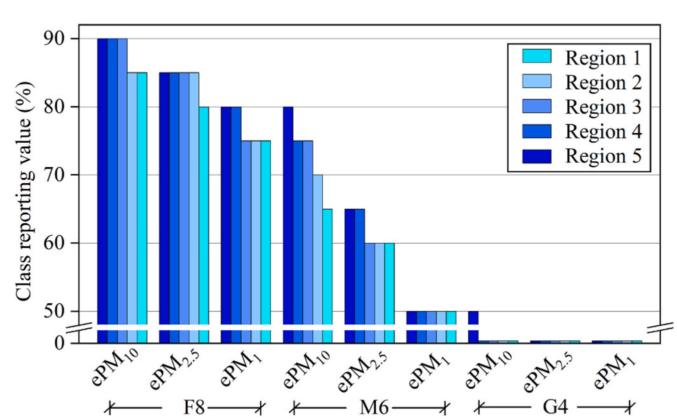

Fig. 14. CRVs of three representative filters with the standardized PSDs.

particulate matter in China is performed based on the national air quality ground observation database, and the fitted curves of the measured PSDs at 35 major cities in China are obtained. The conclusions are as follows:

(1) In the mainland of China, the fine particle proportions ($PM_{2.5}$/PM_{10}) are higher in humid regions and economically developed regions than those in arid regions and nondeveloped regions. The ambient aerosol characteristics vary from region to region evidently.
(2) The PSDs were measured at 35 cities in China, and the results showed that the PSDs of all cities were not the same as those provided by ISO 16890. The mixing ratios, standard deviations and median particle sizes of these PSDs were all different among the cities.
(3) The differences between cities in ePM_X and CRVs of air filters in different regions of China must be addressed due to the differences in ambient aerosol characteristics (i.e., PSDs).
(4) The China PSD regions are divided into five regions and the parameters of these standardized PSDs are determined. It is recommended that air filters for building ventilation, which are marketed and sold to consumers in the mainland of China, should be assessed and classified by their local CRVs in each region.

Author statement

Huayuan Zhou: data curation, formal analysis, software, visualization, writing-original draft, writing-review & editing. **Yang Sun**: data curation, investigation. **Ke Zhong**: conceptualization, methodology, formal analysis. **Yuesi Wang**: aerosol sampling and analysis. **Jie Cai**: investigation. **Yanming Kang**: project administration, supervision, visualization, writing-review & editing.

Data availability statement

The data that support the findings of this study are available from the corresponding author upon reasonable request.

Declaration of competing interest

The authors declare that they have no known competing financial interests or personal relationships that could have appeared to influence the work reported in this paper.

The authors have no conflicts of interest to disclose.

Acknowledgements

This work was supported by the National Natural Science Foundation of China [grant numbers 42075179, 51578121]; the Science and Technology Commission of Shanghai Municipality [grant number 19DZ1205005]; and the Chinese Universities Scientific Fund [grant number CUSF-DH-D-2020075]. The authors would like to thank Dr. D. Gottfried and Dr. Yu Jia for providing valuable comments on the manuscript.

Appendix

Table A.1
Fitting parameters of the measured PSDs at 35 cities

No.	City	y	σ_{gA}	d_{50A}	σ_{gB}	d_{50B}
1	Shanghai	0.93	2.00	0.73	1.25	5.00
2	Hefei	0.88	2.25	0.67	1.55	5.50
3	Harbin	0.79	2.20	0.63	1.45	5.40
4	Nanjing	0.78	2.20	0.62	1.47	5.50
5	Wuhan	0.94	2.04	0.77	1.26	5.50
6	Changsha	0.89	1.99	0.76	1.27	5.60
7	Suzhou	0.88	2.10	0.79	1.25	5.50
8	Chongqing	0.88	2.18	0.80	1.30	5.40
9	Hangzhou	0.83	2.30	0.70	1.50	5.00
10	Tianjin	0.72	2.20	0.62	1.55	6.00
11	Beijing	0.76	2.39	0.78	1.39	5.40
12	Guiyang	0.70	2.10	0.77	1.47	6.30
13	Xiamen	0.72	2.20	0.78	1.34	5.30
14	Fuzhou	0.70	2.19	0.81	1.37	5.70
15	Jinan	0.75	2.38	0.71	1.43	5.30
16	Chengdu	0.66	2.19	0.80	1.54	6.10
17	Nanning	0.70	2.54	0.83	1.50	6.40
18	Qingdao	0.67	2.50	0.75	1.40	5.20
19	Nanchang	0.60	2.38	0.76	1.52	6.70
20	Lanzhou	0.55	2.23	0.73	1.47	5.20
21	Yinchuan	0.60	2.24	0.80	1.66	6.30
22	Shenzhen	0.66	2.10	0.87	1.55	5.80
23	Shenyang	0.68	2.10	0.84	1.50	5.60
24	Guangzhou	0.60	1.80	0.81	1.38	4.80
25	Hohhot	0.70	2.00	0.88	1.39	4.70
26	Changchun	0.85	2.38	1.00	1.28	5.10
27	Shijiazhuang	0.78	2.39	1.03	1.37	5.60
28	Urumqi	0.60	1.97	0.85	1.48	5.00
29	Haikou	0.60	2.00	0.87	1.50	5.40
30	Xining	0.55	1.96	0.87	1.64	5.40
31	Taiyuan	0.58	2.20	0.84	1.57	5.40
32	Xi'an	0.55	1.96	0.87	1.58	5.50
33	Zhengzhou	0.55	1.91	0.87	1.54	5.30
34	Lhasa	0.40	2.04	0.80	1.51	5.50
35	Kunming	0.40	2.04	0.84	1.57	5.50

Table A.2
ePM_X of the three representative filters at 35 cities

No.	City	G4 (%)			M6 (%)			F8 (%)		
		ePM_1	$ePM_{2.5}$	ePM_{10}	ePM_1	$ePM_{2.5}$	ePM_{10}	ePM_1	$ePM_{2.5}$	ePM_{10}
1	Shanghai	16.3	23.6	27.5	53.2	61.6	65.0	79.8	84.8	86.2
2	Hefei	16.0	23.9	30.2	52.5	61.6	66.8	79.3	84.7	86.8
3	Harbin	16.0	23.3	33.8	52.2	60.8	69.4	79.2	84.2	87.8
4	Nanjing	15.9	23.1	34.1	52.2	60.6	69.5	79.1	84.1	87.8
5	Wuhan	16.4	24.4	28.1	53.4	62.6	65.6	79.9	85.4	86.6
6	Changsha	16.4	23.9	29.8	53.3	62.0	66.7	79.9	85.1	87.0
7	Suzhou	16.4	24.8	31.4	53.4	63.1	68.4	79.9	85.6	87.8
8	Chongqing	16.3	25.2	32.0	53.3	63.4	69.0	79.9	85.8	88.1
9	Hangzhou	16.1	24.7	33.0	52.6	62.6	69.4	79.4	85.2	88.0
10	Tianjin	16.0	24.6	37.1	52.4	62.3	72.3	79.3	85.0	89.2
11	Beijing	16.2	25.5	37.9	52.9	63.7	73.5	79.6	85.9	89.9
12	Guiyang	16.3	24.8	38.7	53.3	63.0	73.6	79.9	85.6	89.8
13	Xiamen	16.3	25.1	38.5	53.1	63.3	74.0	79.8	85.7	90.1
14	Fuzhou	16.3	25.5	39.9	53.3	63.8	75.0	79.9	86.0	90.5
15	Jinan	16.3	26.0	40.0	53.2	64.3	75.2	79.9	86.2	90.6
16	Chengdu	16.3	25.7	40.6	53.3	64.0	75.4	79.9	86.1	90.6
17	Nanning	16.2	26.3	41.3	53.0	64.5	75.9	79.7	86.3	90.9
18	Qingdao	16.1	25.7	41.5	52.7	63.8	76.4	79.5	85.9	91.1
19	Nanchang	16.2	25.5	44.0	52.8	63.6	77.5	79.6	85.8	91.4
20	Lanzhou	16.2	25.8	44.5	52.8	63.9	78.7	79.6	85.9	92.0
21	Yinchuan	16.3	26.3	42.4	53.2	64.6	76.8	79.9	86.4	91.2
22	Shenzhen	16.5	26.6	40.6	53.4	63.8	75.0	80.0	86.0	90.5
23	Shenyang	16.5	26.1	39.8	53.7	64.6	75.1	80.2	86.5	90.7
24	Guangzhou	16.7	25.2	40.6	54.4	63.9	76.2	80.7	86.2	91.2
25	Hohhot	16.7	26.5	39.2	54.3	65.3	75.3	80.6	86.9	90.9
26	Changchun	16.7	27.8	39.3	54.3	66.7	75.5	80.7	87.7	91.1
27	Shijiazhuang	16.5	27.9	39.8	53.9	66.6	75.8	80.3	87.6	91.2
28	Urumqi	16.6	26.7	41.8	54.1	65.3	77.2	80.5	86.9	91.6
29	Haikou	16.6	26.7	42.5	54.1	65.4	77.5	80.5	87.0	91.7
30	Xining	16.7	27.5	43.3	54.2	66.3	78.2	80.6	87.4	92.0
31	Taiyuan	16.4	27.1	43.5	53.5	65.6	78.2	80.1	86.9	91.9
32	Xi'an	16.7	27.1	43.8	54.2	65.9	78.5	80.6	87.2	92.1
33	Zhengzhou	16.7	27.0	43.7	54.4	65.9	78.5	80.8	87.2	92.2
34	Lhasa	16.4	27.0	50.2	53.6	65.4	83.1	80.1	86.8	93.8
35	Kunming	16.5	27.6	50.2	53.8	66.3	83.2	80.3	87.3	93.9

Table A.3
The provinces (cities) in each PSD region

China PSD region	Province (City)
Region 1	Shanghai (Shanghai)
	Hubei (Wuhan)
	Anhui (Hefei)
	Hunan (Changsha)
	Jiangsu (Nanjing, Suzhou)
	Chongqing (Chongqing)
	Heilongjiang (Harbin)
	Zhejiang (Hangzhou)
Region 2	Tianjin (Tianjin)
	Beijing (Beijing)
	Guizhou (Guiyang)
	Fujian (Fuzhou, Xiamen)
Region 3	Guangdong (Guangzhou, Shenzhen)
	Liaoning (Shenyang)
	Shandong (Jinan, Qingdao)
	Sichuan (Chengdu)
	Guangxi (Nanning)
	Ningxia (Yinchuan)
	Jiangxi (Nanchang)
	Gansu (Lanzhou)
Region 4	Inner Mongolia (Hohhot)
	Jilin (Changchun)
	Hebei (Shijiazhuang)
	Xinjiang (Urumqi)
	Hainan (Haikou)
	Qinghai (Xining)
	Shanxi (Taiyuan)
	Shaanxi (Xi'an)
	Henan (Zhengzhou)
Region 5	Tibet (Lhasa)
	Yunnan (Kunming)

References

[1] P.T.B.S. Branco, M.C.M. Alvim-Ferraz, F.G. Martins, S.I. V Sousa, Quantifying indoor air quality determinants in urban and rural nursery and primary schools, Environ. Res. 176 (2019) 108534, https://doi.org/10.1016/j.envres.2019.108534.

[2] E. Zender, – Świercz, Improvement of indoor air quality by way of using decentralised ventilation, J. Build. Eng. 32 (2020) 101663, https://doi.org/10.1016/j.jobe.2020.101663.

[3] H.S. Ganesh, K. Seo, H.E. Fritz, T.F. Edgar, A. Novoselac, M. Baldea, Indoor air quality and energy management in buildings using combined moving horizon estimation and model predictive control, J. Build. Eng. 33 (2021) 101552, https://doi.org/10.1016/j.jobe.2020.101552.

[4] A. Yüksel, M. Arıcı, M. Krajčík, M. Civan, H. Karabay, A review on thermal comfort, indoor air quality and energy consumption in temples, J. Build. Eng. 35 (2021) 102013, https://doi.org/10.1016/j.jobe.2020.102013.

[5] B. Stephens, Evaluating the sensitivity of the mass-based particle removal calculations for HVAC filters in ISO 16890 to assumptions for aerosol distributions, Atmosphere 9 (2018), https://doi.org/10.3390/atmos9030085.

[6] International Organization for Standardization, EN ISO 16890-1: Air Filters for General Ventilation Part 1: Technical Specifications, Requirements and Classification System Based upon Particulate Matter Efficiency, ePM), 2016. https://www.iso.org/standard/57864.html.

[7] National Bureau of Statistics of China, China Statistical Yearbook - 2019, China Statistics Press, Beijing, 2019.

[8] C. Song, L. Wu, Y. Xie, J. He, X. Chen, T. Wang, Y. Lin, T. Jin, A. Wang, Y. Liu, Q. Dai, B. Liu, Y. Wang, H. Mao, Air pollution in China: status and spatiotemporal variations, Environ. Pollut. 227 (2017) 334–347, https://doi.org/10.1016/j.envpol.2017.04.075.

[9] Ministry of Housing and Urban-Rural Development of the People's Republic of China, GB 50176-2016: Thermal Design of Civil Building, 2016. http://www.mohurd.gov.cn/wjfb/201702/t20170213_230579.html.

[10] D. Chen, Y. Zhang, Y. Yao, Y. Hong, Q. Guan, W. Tu, Exploring the spatial differentiation of urbanization on two sides of the Hu Huanyong Line - based on nighttime light data and cellular automata, Appl. Geogr. 112 (2019), https://doi.org/10.1016/j.apgeog.2019.102081.

[11] X. Jinyuan, W. Yuesi, W. Lili, T. Guiqian, S. Yang, P. Yuepeng, J. Dongsheng, Reductions of PM2.5 in beijing-tianjin-hebei urban agglomerations during the 2008 olympic games, Adv. Atmos. Sci. 29 (2012) 1330–1342, https://doi.org/10.1007/s00376-012-1227-4.

[12] H. Patashnick, E.G. Rupprecht, Continuous PM-10 measurements using the tapered element oscillating microbalance, J. Air Waste Manag. Assoc. 41 (1991) 1079–1083, https://doi.org/10.1080/10473289.1991.10466903.

[13] Ministry of Ecology and Environment of the People's Republic of China, HJ/T 193 - 2005: Automated Methods for Ambient Air Quality Monitoring, 2005. http://english.mee.gov.cn/Resources/standards/Air_Environment/air_method/200809/t20080922_129145.shtml.

[14] Y.-L. Zhang, F. Cao, Fine particulate matter (PM2.5) in China at a city level, Sci. Rep. 5 (2015), https://doi.org/10.1038/srep14884.

[15] S. Wang, Y. Li, M. Haque, Evidence on the impact of winter heating policy on air pollution and its dynamic changes in North China, Sustainability 11 (2019), https://doi.org/10.3390/su11102728.

[16] S. Zhao, Y. Yu, D. Yin, J. He, N. Liu, J. Qu, J. Xiao, Annual and diurnal variations of gaseous and particulate pollutants in 31 provincial capital cities based on in situ air quality monitoring data from China National Environmental Monitoring Center, Environ. Int. 86 (2016) 92–106, https://doi.org/10.1016/j.envint.2015.11.003.

[17] H. Fan, C. Zhao, Y. Yang, A comprehensive analysis of the spatio-temporal variation of urban air pollution in China during 2014-2018, Atmos. Environ. 220 (2020), https://doi.org/10.1016/j.atmosenv.2019.117066.

[18] G. D'Amato, L. Cecchi, M. D'amato, G. Liccardi, Urban air pollution and climate change as environmental risk factors of respiratory allergy: an update, J Investig. Allergol. Clin. Immunol. 20 (2010) 95–102.

[19] Y. Pan, Y. Wang, Y. Sun, S. Tian, M. Cheng, Size-resolved aerosol trace elements at a rural mountainous site in Northern China: importance of regional transport, Sci. Total Environ. 461 (2013) 761–771, https://doi.org/10.1016/j.scitotenv.2013.04.065.

[20] J.H. Seinfeld, S.N. Pandis, Atmospheric Chemistry and Physics: from Air Pollution to Climate Change, 2 nd, John Wiley & Sons Inc., New York, 2016.

[21] R. Jaenicke, C. Junge, Studien zur oberen Grenzgröße des natürlichen Aerosols, Beitr. Phys. Atmos. 40 (1967) 129–143.

[22] K.T. Whitby, The physical characteristics of sulfur aerosols, Atmos. Environ. 12 (1978) 135–159, https://doi.org/10.1016/0004-6981(78)90196-8.

[23] P.V. Hobbs, Aerosol-Cloud-Climate Interactions, Academic Press, New York, 1993.

[24] P. V Hobbs, D.A. Bowdle, L.F. Radke, Particles in the lower troposphere over the high plains of the United States. Part I: size distributions, elemental compositions and morphologies, J. Clim. Appl. Meteorol. 24 (1985) 1344–1356, https://doi.org/10.1175/1520-0450(1985)024<1344:PITLTO>2.0.CO;2.

[25] H. Che, H. Zhao, X. Xia, Y. Wu, J. Zhu, Y. Ma, Y. Wang, H. Wang, Y. Wang, X. Zhang, G. Shi, Fine mode aerosol optical properties related to cloud and fog processing over a cluster of cities in Northeast China, Aerosol Air Qual. Res. 15 (2015) 2065–2081, https://doi.org/10.4209/aaqr.2014.12.0325.

[26] J. Hao, Y. Yin, X. Kuang, J. Chen, L. Yuan, H. Xiao, Z. Li, M. Pu, J. Wang, X. Zhou, Y. Chen, Y. Wu, Aircraft measurements of the aerosol spatial distribution and relation with clouds over Eastern China, Aerosol Air Qual. Res. 17 (2017) 3230–3243, https://doi.org/10.4209/aaqr.2016.12.0576.

[27] L. Chen, J. Mao, H. Zhao, C. Zhou, X. Gong, Size distribution and concentration of aerosol particles in Yinchuan area, China, Phys. Geogr. 40 (2019) 538–553, https://doi.org/10.1080/02723646.2019.1613325.

[28] International Organization for Standardization, EN ISO 16890-4: Air Filters for General Ventilation Part 4: Conditioning Method to Determine the Minimum Fractional Test Efficiency, 2016. https://www.iso.org/standard/57867.html.

[29] J.E. Yit, B.T. Chew, Y.H. Yau, A review of air filter test standards for particulate matter of general ventilation, Build. Serv. Eng. Technol. 41 (2020) 758–771, https://doi.org/10.1177/0143624420915626.

Nomenclature

PM: Particulate matter
IAQ: Indoor air quality
ePM_X: Efficiency of PM with an optical diameter between 0.3 μm and *X* μm
PSD: Particle size distribution
CRV: Class reporting value
NAQMS: National air quality monitoring site
FPP: Fine particle proportion
MP: Median of fine particle proportion
d: Optical diameter (μm)
C_{10}: Mass concentrations of PM_{10} (μg/m^3)
$C_{2.5}$: Mass concentrations of $PM_{2.5}$ (μg/m^3)
$q_i(d)$: Actual particle mass frequencies *versus* cut-off diameters (%)
i: Number of the channel (size range) of the impactor
m_i: PMmass concentrations (μg/m^3) in the channel *i*
M: Total PM mass concentrations (μg/m^3)
q(d): Particle mass frequencies (%)
y: Mixing ratio
d_{50}: Median optical diameters (μm)
E_i: Initial size-resolved removal efficiency curve (%)
$E_{D,i}$: Size-resolved removal efficiency curve (%)
$E_{A,i}$: Average size-resolved removal efficiency curve (%)
$\overline{d}_i$: Geometric mean diameter (μm)
n: Number of the channel (size range) which includes the particle size
$ePM_{2.5,min}$: Minimum efficiencies of PM with an optical diameter between 0.3 μm and 2.5 μm
$ePM_{1,min}$: Minimum efficiencies of PM with an optical diameter between 0.3 μm and 1 μm
Greek symbols
η_f: Fine particle proportion
η_m: Median of fine particle proportion
σ_g: Standard deviation